Available online at www.sciencedirect.com
SCIENCE DIRECT®
Journal of Molecular Catalysis A: Chemical 240 (2005) 239–244
JOURNAL OF MOLECULAR CATALYSIS A: CHEMICAL
www.elsevier.com/locate/molcata

MCM-41 and SBA-15 supported Cp_2ZrCl_2 catalysts for the preparation of nano-polyethylene fibres via in situ ethylene extrusion polymerization

Xiaochen Dong, Li Wang *, Guohua Jiang, Zhenrong Zhao, Tianxu Sun, Haojie Yu, Wenqin Wang

The State Key Laboratory of Polymer Reaction Engineering, College of Materials Science and Chemical Engineering, Zhejiang University, Hangzhou 310027, China

Received 7 January 2005; received in revised form 23 June 2005; accepted 29 June 2005
Available online 10 August 2005

Abstract

Under atmospheric pressure, nano-polyethylene fibres were prepared via in situ ethylene extrusion polymerization, with MCM-41 and SBA-15 supported zirconocene dichloride (Cp_2ZrCl_2) catalytic systems, respectively. The effects of the geometrical structures and surface properties of MCM-41 and SBA-15 on the morphology of the resultant polyethylene, catalytic activity and polymerization rate were investigated and compared in various polymerization conditions. The possible formation mechanism of nano-polyethylene fibres with MCM-41 and SBA-15 supported Cp_2ZrCl_2 as catalyst was discussed.

Keywords: MCM-41 and SBA-15; Ethylene polymerization; Nano-polyethylene fibres; Atmospheric pressure

1. Introduction

Recently, a large number of researches, about heterogeneous metallocene catalysts supported on inorganic and organic materials, have been published [1–7]. The discovery of the M41S family of mesoporous zeolites has greatly increased the range of supports for preparing heterogeneous catalysts. MCM-41 and SBA-15 have regular, cylindrical, ordered hexagonal pores, with narrow pore size distribution and large surface area [8,9]. Their pore diameters are larger (2–10 nm) compared to common zeolites, enabling large metallocene molecules to be immobilized not only onto the surface but also inside the pores of the supports. Braca et al. [10] and Michellotti et al. [11] reported that mesoporous zeolites were suitable supports due to the possibility of entrapping organometallic complexes in their large mesoporous channels. Furthermore, the geometrical shape of the nano-channels can serve as polymerization reactors to affect the pattern of monomer insertion and to control polymer chain structure, polymer chains arrangement and polymer morphology. Aida and co-workers [12] first synthesized crystalline line polyethylene nano-fibres with MSF supported titanocene dichloride (Cp_2TiCl_2) catalysts at ethylene pressure 10 atm, and termed as extrusion polymerization. Ye et al. [13] also prepared PE nano-fibres with MCM-41 supported Cp_2TiCl_2 at higher ethylene pressure (20 atm).

In this work, nano-polyethylene fibres were prepared via in situ ethylene extrusion polymerization with Cp_2ZrCl_2 immobilized on MCM-41 and SBA-15 under atmospheric pressure. The influence of structure of MCM-41 and SBA-15 and the different polymerization conditions on the morphology of the resultant polyethylene fibres and catalytic activities were investigated and compared in detail.

* Corresponding author. Tel.: +86 571 8795 3200; fax: +86 571 8795 1612.
E-mail address: opl_wl@dial.zju.edu.cn (L. Wang).

1381-1169/$ – see front matter © 2005 Elsevier B.V. All rights reserved.
doi:10.1016/j.molcata.2005.06.060

2. Experimental

2.1. Materials

All manipulations were carried out by the standard Schlenk technique under argon atmosphere. Zirconocene dichloride (Cp_2ZrCl_2) was synthesized according to the literature [14]. MAO was purchased from Aldrich as 10 wt% aluminium solution in toluene. Polymerization-grade ethylene was purified using three columns of KOH, CuO and 4A molecular sieve. Toluene was refluxed over sodium with benzophenone as indicator and distilled under argon atmosphere before use.

2.2. Preparation of the MCM-41 and SBA-15 supported catalysts

MCM-41 and SBA-15 were synthesized by methods analogous to those reported in literatures [15,16]. The resultant white precipitate was filtrated, washed and calcined in air at 550 °C for 5 and 8 h, respectively. The weighed MCM-41 or SBA-15 was mixed with MAO in 50 ml toluene. After being stirred for 2 h at room temperature, the solid was collected and washed three times with toluene. Subsequently, the MAO pretreated sample was mixed with stoichiometrical amount of Cp_2ZrCl_2 in 50 ml toluene. After being stirred for 1 h at 50 °C, the resultant solid was collected and washed three times with fresh toluene. The supported catalyst was dried in vacuum at room temperature. Spectrophotometric analysis was used to measure the supported Zr amount on MCM-41 and SBA-15, respectively.

2.3. Ethylene extrusion polymerization

Under atmospheric pressure, ethylene extrusion polymerization was carried out in a 100 ml flask equipped with an ethylene inlet, a magnetic stirrer and connected to vacuum line. At selected polymerization temperature, toluene was introduced into the flask and saturated with ethylene, then were added the required MAO and supported catalyst. The polymerization was terminated at a fixed time by adding acidified ethanol. The polymer was separated by filtration and dried under vacuum to constant weight.

2.4. Characterization of the resultant polyethylene

The melting points (T_m) of polyethylene were measured with a Perkin-Elmer DSC-7 differential scanning calorimeter (DSC). The polyethylene sample (ca. 4 mg) was heated to 170 °C at a heating rate of 10 °C/min. Polyethylene morphology was evaluated with scanning electron microscopy (SIRION, FEI, USA). The X-ray powder diffraction (XRD) patterns of polyethylene were obtained on a D/max-3BX diffractometer using Cu Kα radiation of wavelength 0.154 nm.

Table 1
Structural parameters of MCM-41 and SBA-15 samples

Support	S_{BET} (m^2/g)	d_p (Å)	V_p (ml/g)	d_{100} (Å)	b_p (Å)
MCM-41	1082	29.0	0.79	41	9.2
SBA-15	545	56.4	0.77	102	30.7

S_{BET}, BET specific surface area; V_p, specific pore volume; d_p, average pore diameter, obtained from BJH adsorption data, $d_p = 4V_p/S_{BET}$; d_{100}, XRD interplanar spacing; b_p, pore wall thickness, $b_p = (a_0 - d_p)/2$, $a_0 = (2/\sqrt{3})d_{100}$.

3. Results and discussion

3.1. Characterization of MCM-41 and SBA-15

MCM-41 and SBA-15 samples with different pore diameter and surface properties were used as supports for Cp_2ZrCl_2 catalysts in this work. MCM-41 and SBA-15 have been studied extensively by our group [17,18]. The structural parameters of the MCM-41 and SBA-15 samples are listed in Table 1.

Both MCM-41 and SBA-15 have narrow pore diameter distribution, as shown in Fig. 1.

3.2. Ethylene polymerization and polyethylene characterization

Under atmospheric pressure, ethylene polymerization was carried out with MCM-41 and SBA-15 supported catalytic systems. Table 2 listed the polymerization reaction conditions, polymerization activity and melting points of the resultant polyethylene.

3.2.1. Effect of supports on polymerization activities

The activities of the MCM-41 and SBA-15 supported catalytic systems for ethylene polymerization were about 30% of those of the homogeneous system (Table 2). Similar results had been reported elsewhere [19]. This could be attributed to the deactivation of some of the active sites on reaction

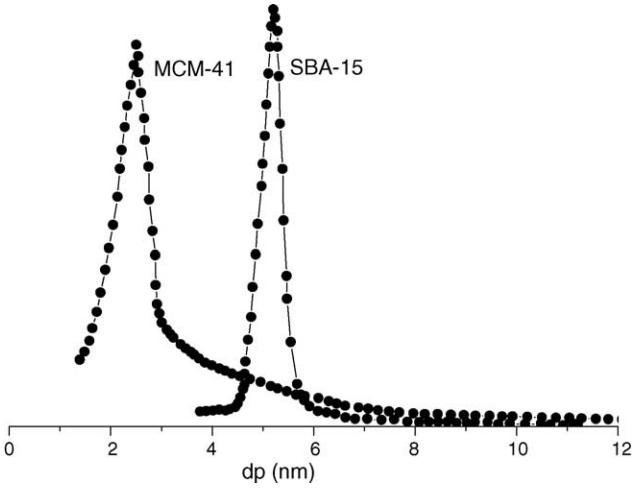

Fig. 1. Pore diameter distribution of MCM-41 and SBA-15.

Table 2
The results of ethylene polymerization catalyzed by supported catalysts and homogeneous catalyst[a]

Run	Catalysts	Temperature (°C)	[Al]/[Zr]	Activity[b]	T_m (°C)	ΔH (J/g)
1	Cp_2ZrCl_2/MCM-41	30	2000	0.38	136.0	212.4
2		50	2000	0.49	134.0	204.1
3		70	2000	1.74	130.4	200.7
4	Cp_2ZrCl_2/SBA-15	30	2000	0.33	134.7	197.9
5		50	2000	0.53	129.8	208.3
6		70	2000	0.90	128.8	207.0
7	Cp_2ZrCl_2	50	2000	1.54	129.7	197.9

[a] Polymerization conditions: toluene = 50 ml, ethylene pressure = 1 atm, t = 30 min.
[b] $\times 10^6$ g PE/(mol Zr h atm).

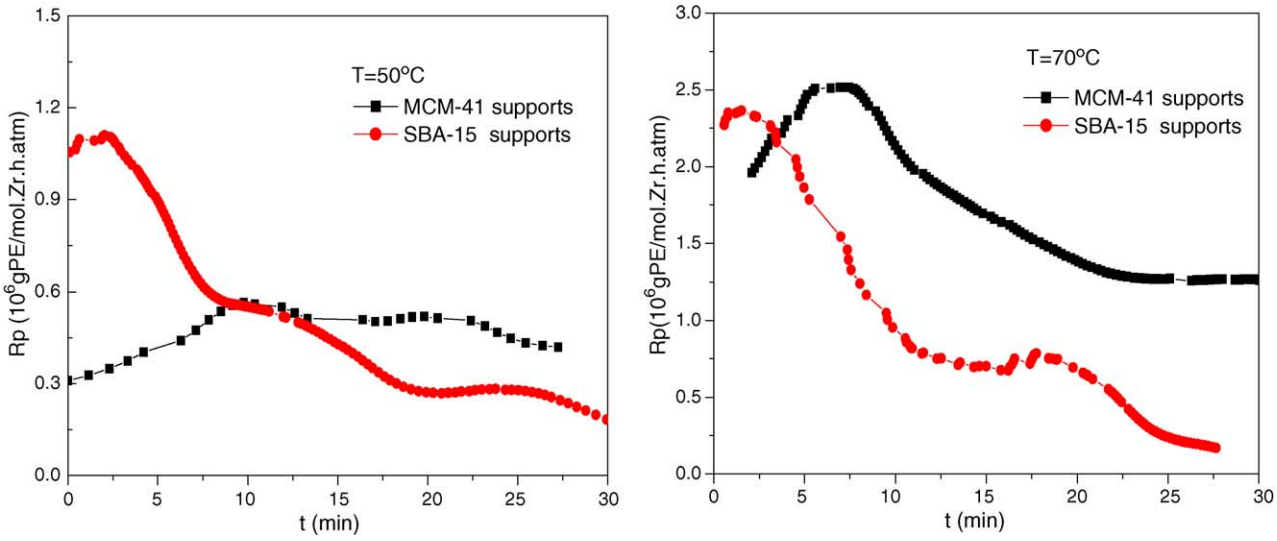

Fig. 2. The influence of supports on the ethylene polymerization rate. Polymerization conditions: [Al]/[Zr] = 2000, toluene = 50 ml.

with MCM-41 and SBA-15 and could also owe to the steric hindrance in the pore of MCM-41 and SBA-15. The polymerization activities increased drastically with the increase in the reaction temperature. The activities of the two heterogeneous catalytic systems were similar. The influences of supports on the ethylene polymerization rate are shown in Fig. 2. It was believed that the difference in the polymerization rate for the MCM-41 and SBA-15 supported catalysts was due to the difference in the pore diameters and surface areas.

3.2.2. Effect of supports on melting points of polyethylene

The melting points of the polyethylene prepared by supported catalytic system, particularly MCM-41 supported catalysts, were higher than those of the corresponding homogeneous catalytic system. This is probably attributed to the control of channels over the arrangement of polyethylene chains. The channel diameter of mesoporous sieves (29 and 56.4 Å) is smaller than the lamellar thickness (270 Å) of the folded-chain crystals of ordinary polyethylene [20]. When the ethylene monomers pass into the channel, the wall of the channel can control the direction of ethylene propagation, form polyethylene extended-chains and then form extended-chains crystals. The extended-chains crystals are beneficial to increasing the melting points. The schematic illustration of the process is shown in Fig. 3.

The melting points of polyethylene prepared by MCM-41 supported catalysts were higher than those prepared by

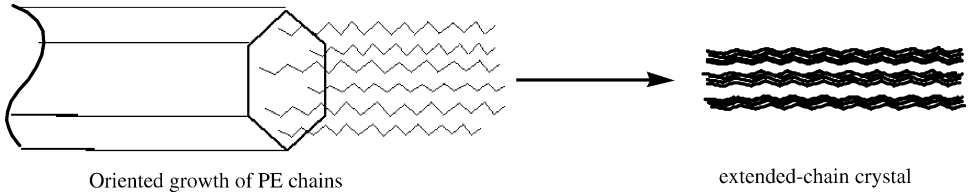

Fig. 3. The schematic illustration for the formation process of extended-chains crystals.

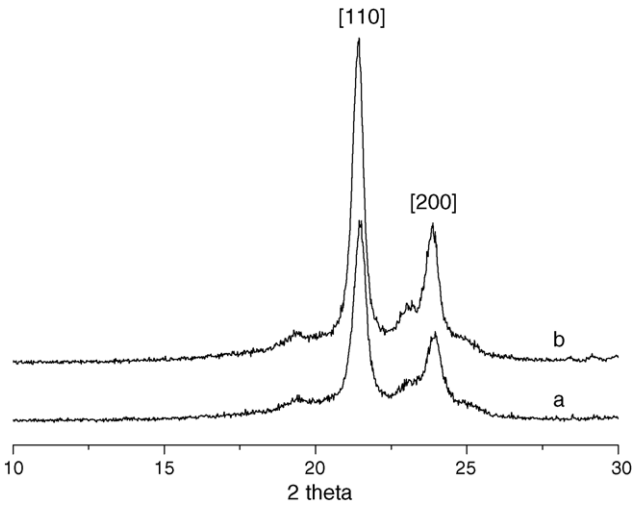

Fig. 4. XRD patterns of PE (a) prepared with MCM-41 supported catalyst, (b) prepared with SBA-15 supported catalysts ([Al]/[Zr] = 2000, $T = 50\,^{\circ}C$, $t = 30$ min).

SBA-15 supported catalysts. It is reasonable that this is attributed to the difference in the pore diameter between MCM-41 and SBA-15. Firstly, SBA-15 with larger pore diameter is not easy to control the chains structure thoroughly to obtain complete extended-chains; secondly, some extended-chains are not controlled very well by the channels and can change to folded-chains again without crystallizing.

Fig. 4 shows the XRD patterns of the polyethylene samples prepared with MCM-41 and SBA-15 supported catalytic systems. Typical orthorhombic crystal structure for the crystalline PE with [1 1 0] and [2 0 0] diffraction peaks at 21.2° and 24°, respectively, testifies the existence of extended-chains crystals [13]. The small amorphous halo around 19.4°, particularly the sample prepared with SBA-15 supported catalyst, indicates the existence of folded-chains.

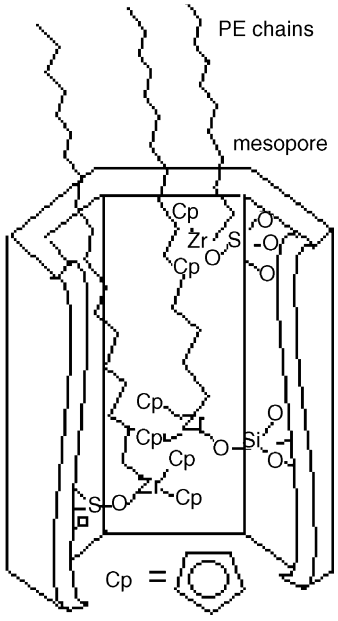

Fig. 6. Scheme for the formation of PE nano-fibres through mesoporous channel.

3.3. Morphology of the resultant polyethylene

3.3.1. Effect of the supports on the morphology of the resultant polyethylene

The morphologies of the resultant polyethylene were studied with SEM in detail. Fig. 5(a and b) shows the SEM micrographs of polyethylene prepared by MCM-41 and SBA-15 supported catalytic systems for 10 min, respectively. It is clear that, owing to the control of the channels of MCM-41 and SBA-15 over the polyethylene chains, the resultant polyethylene presents nano-fibre morphologies with smooth surface.

Fig. 6 shows the scheme for the formation of the nano-fibres through mesoporous channel [12].

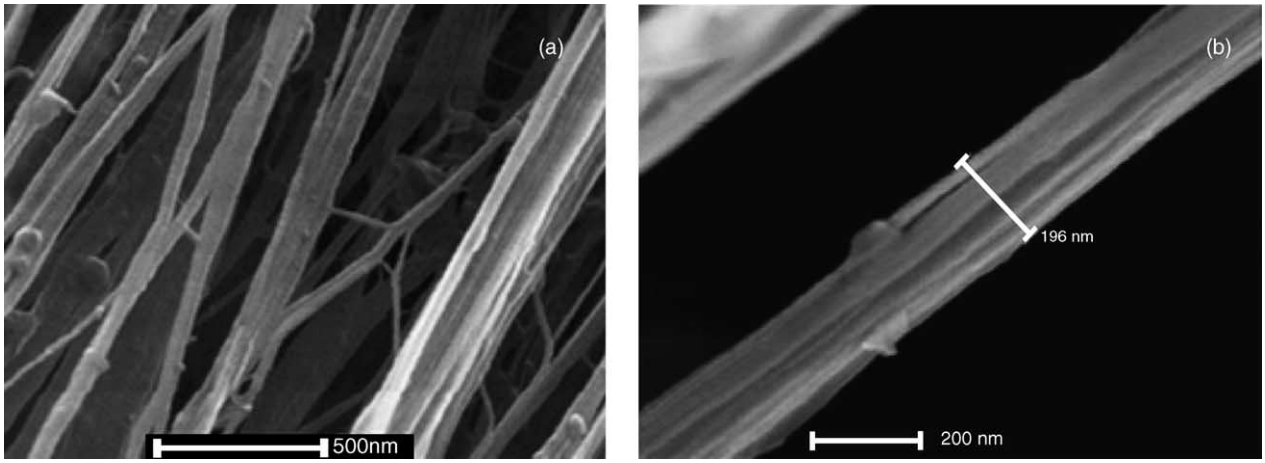

Fig. 5. SEM micrographs of polyethylene fibres prepared by heterogeneous catalytic systems ([Al]/[Zr] = 2000, $T = 50\,^{\circ}C$, $t = 10$ min): (a) MCM-41 supported catalytic system and (b) SBA-15 supported catalytic system.

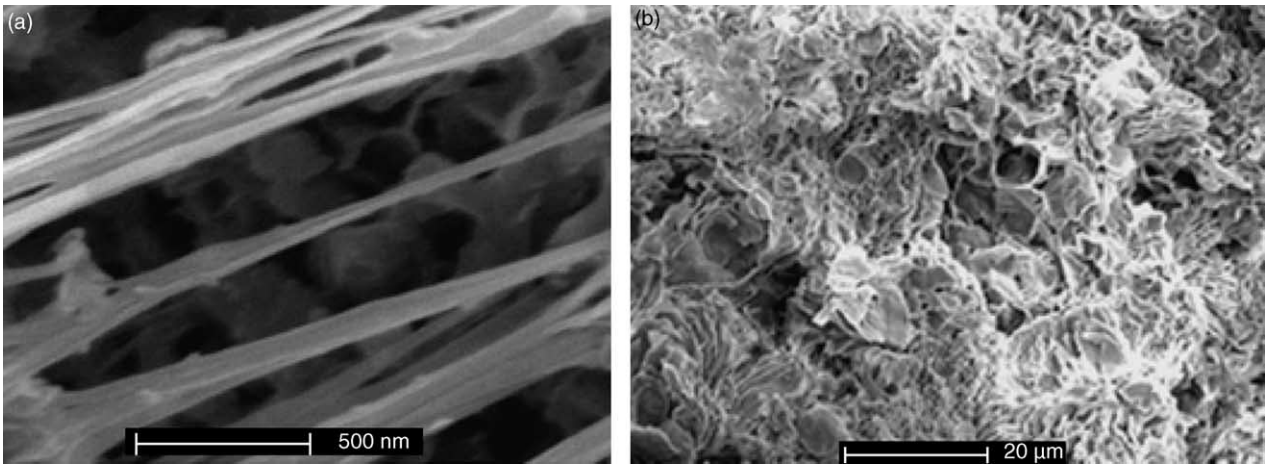

Fig. 7. SEM micrographs of polyethylene prepared with supported catalytic systems at $T = 70\,^{\circ}C$ ([Al]/[Zr] = 2000, $t = 30$ min): (a) MCM-41 supported catalytic system and (b) SBA-15 supported catalytic system.

Comparison between Fig. 5(a and b) indicates that the nano-fibres prepared by SBA-15 are larger in diameter than those prepared by MCM-41 supported catalyst. This result is due to the difference in the pore diameter between SBA-15 and MCM-41. SBA-15 has larger pore diameter than MCM-41, containing more polyethylene chains in the pore.

3.3.2. Effect of polymerization temperature on the morphology of the resultant polyethylene

In order to explore how the polymerization temperature affects the polymer morphology, we also observed the morphology of the resultant polyethylene prepared with SBA-15 and MCM-41 supported catalytic systems at 70 °C, as shown in Fig. 7. The fibre morphology can be observed in the polyethylene prepared by MCM-41 supported catalyst, while the polyethylene prepared by SBA-15 supported catalyst presents non-fibre morphology. Possible reason is that with the increase in polymerization temperature, the polymerization rate increases. With the propagation of polyethylene chains, the framework of MCM-41 could keep the original channel structure. The channels could control the chains inside the pore and form polyethylene fibres (Fig. 7(a)). SBA-15 channels have larger diameter and may contain more polyethylene chains than MCM-41, which make the SBA-15 channels broken into small particles under high polymerization rate. Therefore, the polyethylene may follow the so-called replica phenomenon and resembles the broken support particles (Fig. 7(b)).

4. Conclusions

Under atmospheric pressure, nano-polyethylene fibres can be prepared via ethylene extrusion polymerization in situ with MCM-41 and SBA-15 supported Cp_2ZrCl_2 catalytic systems. The diameters of the resultant fibres prepared with SBA-15 supported catalysts are larger than those prepared with MCM-41 supported catalysts. At the polymerization temperature of 70 °C, the fibre morphology of the polyethylene prepared with SBA-15 supported catalytic system disappeared. Furthermore, the resultant polyethylene had higher melting points compared to the homogeneous counterpart, particularly the samples prepared with MCM-41 supported catalysts.

Acknowledgements

This work is supported by National Nature Science Foundation of China (20172045). The authors also thank Luo Yongming for the help of preparation and characterization of MCM-41 and SBA-15.

References

[1] K. Soga, H.J. Kim, T. Shiono, Macromol. Chem. Phys. 195 (1994) 3347.
[2] I.N. Meshkova, T.M. Vshakova, T.A. Ladygina, et al., Polym. Bull. 44 (2000) 461.
[3] F.H. Meng, G.Q. Yu, B.T. Huang, J. Polym. Sci., Part A: Polym. Chem. 37 (1999) 37.
[4] G. Satyanarayana, S. Sivaram, Macromolecules 26 (1993) 4712.
[5] S.C. Hong, H.T. Ban, N. Kishi, J. Jin, T. Uozumi, K. Soga, Macromol. Chem. Phys. 199 (1998) 1393.
[6] S.C. Hong, T. Teranishi, K. Soga, Polymer 39 (1998) 7153.
[7] H. Nishida, T. Uozomi, T. Arai, K. Soga, Macromol. Chem. Rapid Commun. 16 (1995) 821.
[8] C.T. Kresge, M.E. Leonowicz, W.J. Roth, J.C. Vartuli, J.S. Beck, Nature 359 (1992) 710.
[9] J.S. Beck, J.C. Vartuli, W.J. Roth, M.E. Leonowicz, C.T. Kresge, K.D. Schmitt, C.T.W. Chu, D.H. Olson, E.W. Sheppard, S.B. McCullen, J.B. Higgins, J.L. Schlenker, J. Am. Chem. Soc. 114 (1992) 10834.
[10] G. Braca, G. Sbran, A.M. Raspolli, A. Altomare, G. Arribas, M. Michelotti, F. Ciardelli, J. Mol. Catal. A: Chem. 107 (1996) 113.
[11] M. Michellotti, A. Altomare, F. Ciardelli, E. Roland, J. Mol. Catal. A: Chem. 129 (1998) 241.
[12] K. Kageyama, J.I. Tamazawa, T. Aida, Science 285 (24) (1999) 2113.

[13] Z.B. Ye, S.P. Zhu, W.J. Wang, H. Alsyouri, Y.S. Lin, J. Polym. Sci., Part B: Polym. Phys. 41 (2003) 2433.
[14] R.B. King, Organometallic Chemistry of Transition Metal, Academic Press, 1981.
[15] M. Grun, K.K. Unger, A. Matsumoto, K. Tsutsumi, Microporous Mesoporous Mater. 27 (1999) 207.
[16] D.Y. Zhao, J.L. Feng, Q.S. Huo, Science 279 (1998) 548.
[17] X.C. Dong, L. Wang, W.Q. Wang, H.J. Yu, J.F. Wang, T. Chen, Z.R. Zhao, Eur. Polym. J. 41 (2005) 797.
[18] X.C. Dong, L. Wang, W.Q. Wang, G.H. Jiang, Y. Chen, Z.R. Zhao, J.J. Wang, Macromol. Mater. Eng. 290 (2005) 31.
[19] K.S. Lee, C.G. Oh, J.H. Yim, S.K. Ihm, J. Mol. Catal. A: Chem. 159 (2000) 301.
[20] K. Tajima, T. Aida, Chem. Commun. 24 (2000) 2399.